Structure-Activity-Relationship Exploration and Animal Validation of Novel Assembly Modulator Small Molecule Chemical Series with Pan-Cancer Selective Cytotoxicity

Authors

Anuradha F. Lingappa[1], Suguna Mallesh[1], Maya Michon[1], Devaraju Shivarudraswamy[1], Jim Lin[1], Dharma Prasad[1], Debendranath Dey[1], Dennis Solas[1], Vishwanath R. Lingappa[1,2,3]

[1] Prosetta Biosciences, Inc. 670 5th St San Francisco, CA 94107

[2] University of California, San Francisco

[3] To whom correspondence should be addressed.

Abstract

A novel class of protein assembly modulator chemical compounds that exhibit broad anti-tumor cytotoxicity has been recently described. Here we present a more detailed structure-activity-relationship exploration of the chemical series. PAV-0805, an advanced analog, was found to be safe in mice at 10mg/kg and nontoxic to normal human peripheral blood mononuclear cells (PBMC) cells. PAV-0805 has demonstrated broad anti-cancer activity in the NCI-60 cell lines, including against a diversity of brain, breast, colon, lung, ovarian prostate, renal, and skin cancers, and leukemias. In the aggressive 4T1 mouse allograft breast cancer model, PAV-0805 was effective in reducing tumor growth and metastasis when treatment was initiated early (primary tumor volume of $50mm^3$) or late (primary tumor volume of $500mm^3$), and under both treatment conditions showed inhibition of both tumor growth and metastasis comparable to paclitaxel. The novel multi-protein complex targeted by these compounds is enriched in gene products involved in the cancer hallmarks of resisting cell death and reprogramming energy metabolism.

Introduction

PAV-951 is a novel small molecule that was originally identified as a modulator of HIV capsid formation in a cell-free protein synthesis and assembly (CFPSA) system[1].

Cell free systems have played an important role in the history of biochemistry and molecular cell biology. Such a system was used in the 19th century to demonstrate that fermentation of sugar to alcohol is possible outside living organisms, in the 1960's to decipher the genetic code, and in the 1970's to prove the signal hypothesis[2–4]. We used CFPSA to reproduce the features of viral capsid formation and then, upon determining that capsid assembly occurs via an energy-dependent, host-catalyzed pathway, repurposed the CFPSA system into a phenotypic screen for identifying antiviral small molecules, by virtue of their inhibition of capsid formation. Advancement of those compounds through medicinal

chemistry has provided evidence that they work through disruption of critical protein-protein interactions at the host-viral interface[5–11]. A benefit of developing a drug screen around CFPSA is that the dimension of protein expression and heterogeneity that occurs after protein synthesis, including post-translational modification and the formation of multi-protein complexes, is preserved and rendered "druggable."

The activity of PAV-951 was validated against infectious HIV in cell culture and then the compound was counterscreened against cancer cell lines[1]. The rationale behind the counterscreen was to use viruses as "trufflehounds" to detect drug targets inaccessible to genomic or conventional proteomic methods[1,12]. While unorthodox, our pursuit of anti-viral compounds for cancer therapeutics has a compelling logic. A vast body of literature draws a connection between viruses and cancer[13–15]. Oncogenic viral proteins facilitate viral propagation and predispose cells to tumorigenesis by various methods, including the disruption or modification of biochemical pathways which are critical for maintaining homeostasis and cell cycle control[15,16].

Human Papilloma Virus (HPV) is a well-known example of an oncogenic virus[15,17]. HPV E7 viral proteins have no known intrinsic enzymatic activities, but they are observed to associate with and modify the functions of cellular protein complexes, with implications for both the virus and the host[15,17–21]. HPV E7 viral protein is itself oncogenic— expression of HPV E7 in a transgenic mouse is sufficient for cervical cancer development[22]. Likewise, in patients with both early and advanced stages of cervical cancer, elevated expression of HPV E7 positively correlates to a high viral load[23]. Since the literature indicates that viruses exploit underlying weak links in cellular homeostasis as a means of hijacking host protein machinery to facilitate capsid assembly, we hypothesized that our compounds which normalize protein-protein interactions at the host-viral interface may also restore homeostasis, including the restoration of diverse subcellular controls leading to programmed cell death, in neoplastic cells[1].

PAV-951, the initial compound identified through our unique approach as both anti-viral *and* anti-cancer, displays a number of unique properties. First, its anti-cancer activity appears to be pan-cancer[1]. Anti-cancer properties were observed against 80 of 80 different tumor cell lines and in two mouse

xenograft studies on lung and colon cancer[1], although the degree of efficacy varied substantially among the cancers tested. Second, its anti-cancer potency appears to be an order of magnitude improved when added to trypsinized cells at the time of plating, rather than to cells which have adhered to their growth matrix— conditions which model metastasis and suggest relevance to the epithelial-to-mesenchymal transition[1]. Third, its target appears to be a dynamic multi-protein complex[1]. This third observation was gleaned from drug resin affinity chromatography (DRAC) experiments conducted in the presence of metabolic energy. In the DRAC experiments, PAV-951 was modified from a biologically irrelevant position which allowed it to be coupled to an affi-gel resin. The resin was incubated with cancer cell extract, washed to remove non-specifically bound proteins, and then the remaining resin-bound proteins were eluted with free compound. The DRAC eluates contain sets of proteins which migrate together on sucrose gradients[1].

While initial results on PAV-951 display intriguing potential for the development of a novel anti-cancer therapeutic, that is an early compound that remains to be optimized. It shows some degree of activity against all of the NCI-60 screen cancers, but for many of those, activity at 2.5uM PAV-951 is modest[1]. Higher dosing of PAV-951 is limited by toxicity. The maximum tolerated dose (MTD) of PAV-951 in mice was found to be 2.5 mg/kg[1]. To address this and other limitations, chemical analogs of PAV-951 were synthesized.

From earlier work, including on structurally-unrelated assembly modulator compounds active in other therapeutic areas, we hypothesize that the multi-protein complex drug target of PAV-951 is an "assembly machine".[1,5,12,24] Assembly machines in healthy cells are hypothesized to contribute to maintenance of homeostasis[1,5,9,12,24]. Disease advances when assembly machine function, or the normal cellular response to it, is disabled, and has been correlated to a change in the protein composition of the multi-protein complex[1,5,12,24]. In the case of viral infection, the structurally altered multi-protein complex "aberrant assembly machine" is redirected to build a viral capsid, and its ability to trigger host defenses,

silenced[5–9,11,12]. In the case of cancer, the aberrant assembly machine is, directly or indirectly, not adequately responsive to uncontrolled proliferation or another hallmark of cancer[1,12].

Within the framework outlined above, both viruses and cancers take advantage of the patient's underlying assembly machinery and repurpose it for their own ends. An initial hit assembly-modulating compound may cast a wide net in terms of the assembly pathways it targets, and the degree to which it is selective for the aberrant assembly machine. To the extent that it has affinity for the normal assembly machine, assembly modulator drug treatment may cause toxicity due to disruption of biochemical pathways carrying out normal cell function. However, optimization of the chemical series may lead to analogs which are selective for one particular aberrant assembly machine, thereby eliminating only the disease-associated manifestations of disordered protein assembly and avoiding toxicity. Thus, one prediction of this conceptual framework is that optimization of the assembly modulator compound will result in simultaneously improved drug efficacy and greater safety. We have seen for other assembly modulator chemotypes, that it is possible to drive SAR to aberrant assembly machine selectivity[5].

The primary challenge for advancing oncology drugs is how to develop a compound that kills cancer cells and spares normal cells. The potential of our assembly modulating compounds to selectively drug particular biochemical targets/pathways that are associated with disease states (e.g. aberrant assembly machines) rather than inhibiting a target present and functioning in healthy cells, could provide a solution to this challenge. A normal cell which is following its programming for homeostasis would not be affected when exposed to a compound that selectively targets aberrant protein assembly. However, a cancerous cell whose survival requires protein machinery that has departed from homeostasis would experience growth inhibition and/or cytotoxicity when exposed to this compound.

The data to be presented in this paper takes advantage of the superior properties of advanced compounds from our pan-cancer chemical series to achieve this proof-of-concept as well as better understand its target and hypothesized mechanism of action.

Results

Structure-Activity-Relationship Exploration of Pan-Cancer Assembly Modulating Series

Chemical analogs of PAV-951 were assessed in the National Cancer Institute 60 cell line screen (NCI-60). Compounds were tested against up to 60 tumor cell lines (CCRF-CEM, HL-60(TB), K-562, MOLT-4, RPMI-8226, SR, A549/ATCC, EKVX, HOP-62, HOP-92, NCI-H226, NCI-H23, NCI-H322M, NCI-H460, NCI-H522, COLO 205, HCC-2998, HCT-116, HCT-15, HT29, KM12, SW-620, SF-268, SF-295, SF-539, SNB-19, SNB-75, U251, LOX IMVI, MALME-3M, M14, MDA-MB-435, SK-MEL-2, SK-MEL-28, SK-MEL-5, UACC-257, UACC-62, IGROV1, OVCAR-3, OVCAR-4, OVCAR-5, OVCAR-8, NCI/ADR-RES, SK-OV-3, 786-0, A498, ACHN, CAKI-1, RXF 393, SN12C, TK-10, UO-31, PC-3, DU-145, MCF7, MDA-MB-231/ATCC, HS 578T, BT-549, T-47D, MDA-MB-468) at a single dose of 2.5uM. See **Figure 1** for NCI-60 data on PAV-951 and 14 of its chemical analogs.

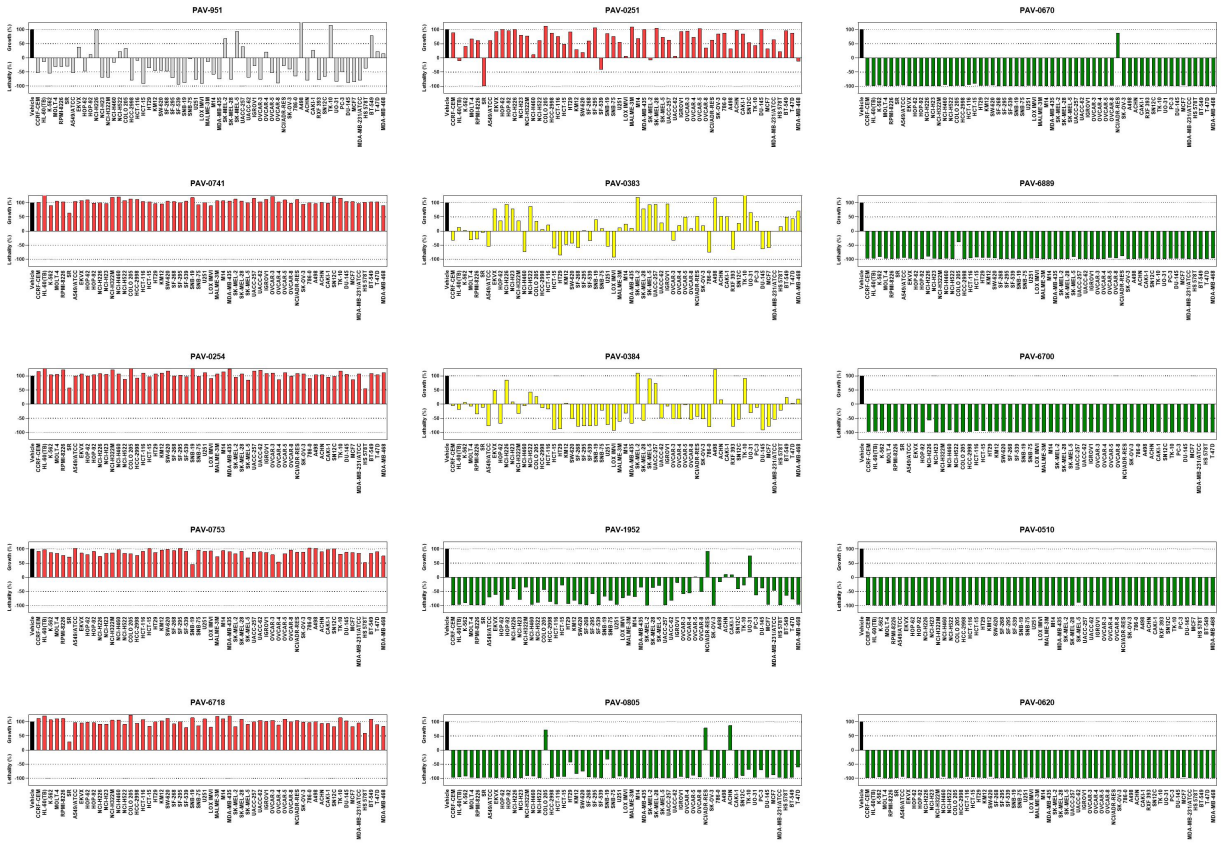

Figure 1. Anti-cancer assessment in the NCI-60 Screen. NCI-60 activity at a single dose of 2.5uM is shown for a set of chemical analogs based on PAV-951. Each bar represents a different tumor cell line. Cell viability of each cancer upon drug treatment is shown relative to the vehicle treated control and number of cells at time 0. Values between 0 and 100 represent percent growth inhibition. Values between 0 and -100 represent percent cellular lethality. Graphs are color coded where red indicates loss, green indicates gain, and yellow indicates no substantial change in the anti-cancer activity of analogs compared to the parent compound.

Safety of active compounds was assessed in Balb/c mice. Increasing doses of compounds were administered to the mice by intraperitoneal (IP) injection. The highest dose which yielded no symptoms of toxicity 24 hours post-dose, was determined to be the MTD. Analogs were identified with 2-4x increases to safety relative to the parent compound, PAV-951. See **Figure 2A** for a table of single-dose mouse MTD.

Two compounds, PAV-0620 and PAV-0805, were assessed in mouse multi-day safety studies. The compound was administered at 10mg/kg daily to three male and three female Balb/c mice. Some mice given PAV-0620 exhibited lethargy on the third day of dosing. Mice given PAV-0805 exhibited no clinical signs of toxicity after 14 days of daily dosing at 10mg/kg.

To gain further insight into the therapeutic window of PAV-0805, it was assessed against non-cancerous peripheral blood mononucleocyte (PBMC) cells and cancerous H9 lymphoma cells, in matched conditions. Cells were seeded at a density of 5,000 cells/well and treated with either DMSO or compound, at concentrations of 2.5uM, 5uM, 10uM, and 20uM. The cells were incubated at 37oC for 72 hours then cell viability was measured using an AlamarBlue™ assay. PAV-0805 did not significantly reduce cell viability in PBMC cells, even at the 20uM dose (See **Figure 2B**). However, PAV-805 showed dose-dependent cytotoxicity to H9 lymphoma (See **Figure 2C**).

A.

Compound	Safe Dose (IP)
PAV-951	<5 mg/kg
PAV-0383	<5 mg/kg
PAV-0384	<5 mg/kg
PAV-0670	<5 mg/kg
PAV-0510	5 mg/kg
PAV-1952	5 mg/kg
PAV-6700	5 mg/kg
PAV-6889	5 mg/kg
PAV-0620	10 mg/kg
PAV-0805	10 mg/kg

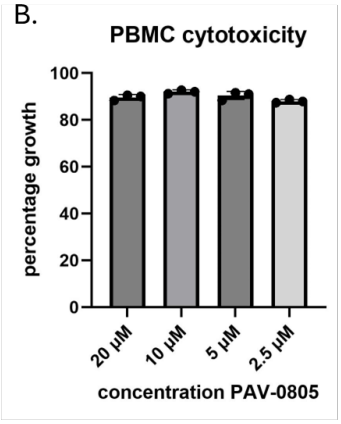

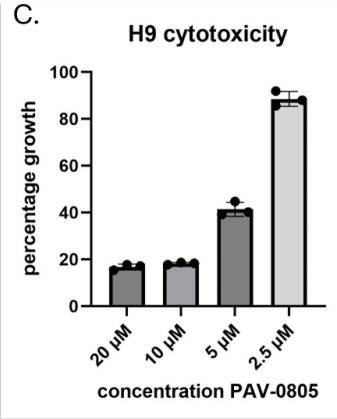

Figure 2. Safety of active chemical analogs. Figure 2A provides a table summarizing mouse safety for PAV-951 and 9 of its active analogs, by the metric of MTD by IP injection. Values are color coded where red indicates compounds that are not significantly safer than the parent compound, yellow indicates compounds that are at approximately 2x safer than the parent compound, and green indicates compounds that are approximately 4x safer than the parent

compound. **Figures 2B** and **2C** show cell viability of normal PBMCs and cancerous lymphoma cells after 72 hours of treatment with 20uM, 10uM, 5uM, or 2.5uM PAV-0805. Graphs show cell viability in treated cells as a percentage of the cell viability measured in DMSO-vehicle treated cells.

Animal Validation of the Advanced Compound PAV-0805

The anti-cancer activity of PAV-0805 was assessed in the 4T1 allograft mouse model. 4T1 is an aggressive triple negative breast cancer that spontaneously metastasizes when implanted into mice[25,26]. After 4T1 cells are implanted , a palpable tumor forms within a week and progresses to a tumor volume of >2,000 mm^3 within 30 days[25,26]. An advantage of using an allograft model, in contrast to the xenograft studies which were used to assess PAV-951, is that the mice are immunocompetent and the interface between a test compound and the immune system are preserved.

A suspension of 0.1×10^6 4T1 cells were implanted into the mammary fat pad of Balb/c mice and tumor size was measured using a digital Vernier caliper. Tumor volume was calculated as the [Length (L) × Width (W) ^{2}] /2, where length (L) is the largest diameter of the tumor and width (W) is the smallest diameter. Tumor growth inhibition was calculated based on the following formula:

$$\% \text{ TGI} = \frac{\{(TV_{vehicle}\text{ Final} - TV_{vehicle}\text{ Initial}) - (TV_{treatment}\text{ Final} - TV_{treatment}\text{ Initial})\}}{(TV_{vehicle}\text{ Final} - TV_{vehicle}\text{ Initial})} \times 100$$

Animals were treated by IP injection daily with either vehicle (N=6), 2 mg/kg Paclitaxel (N=6), or 10mg/kg PAV-0805 (N=6), beginning when the tumor volume reached 50mm^3. An additional late treatment group (N=3) received vehicle until the tumor volume reached 500mm^3, and were subsequently treated with 10mg/kg PAV-0805 daily. Animals were sacrificed once the tumor in the vehicle-treated group reached a volume of 2000mm^3. Upon completion of the study, lung tissues were isolated and visually observed for metastatic cancer cell colonies.

In conditions where treatment began when the tumor was 50mm^3, Paclitaxel inhibited tumor growth by 42% and PAV-0805 inhibited tumor growth by 48% (See **Figure 3A**). When PAV-0805 was administered to a tumor that was at a volume of 500mm^3, it inhibited tumor growth by 38% (See **Figure 3A**). On average 82 lung nodules were found in vehicle-treated animals, 49 lung nodules were found in Paclitaxel-treated animals, 50 lung nodules were found in the PAV-0805 early-treatment group, and 53 lung nodules were found in the PAV-0805 late-treatment group (See **Figure 3B**). PAV-0805 treatment did not substantially impact body weight of the mice (See **Figure 3C**).

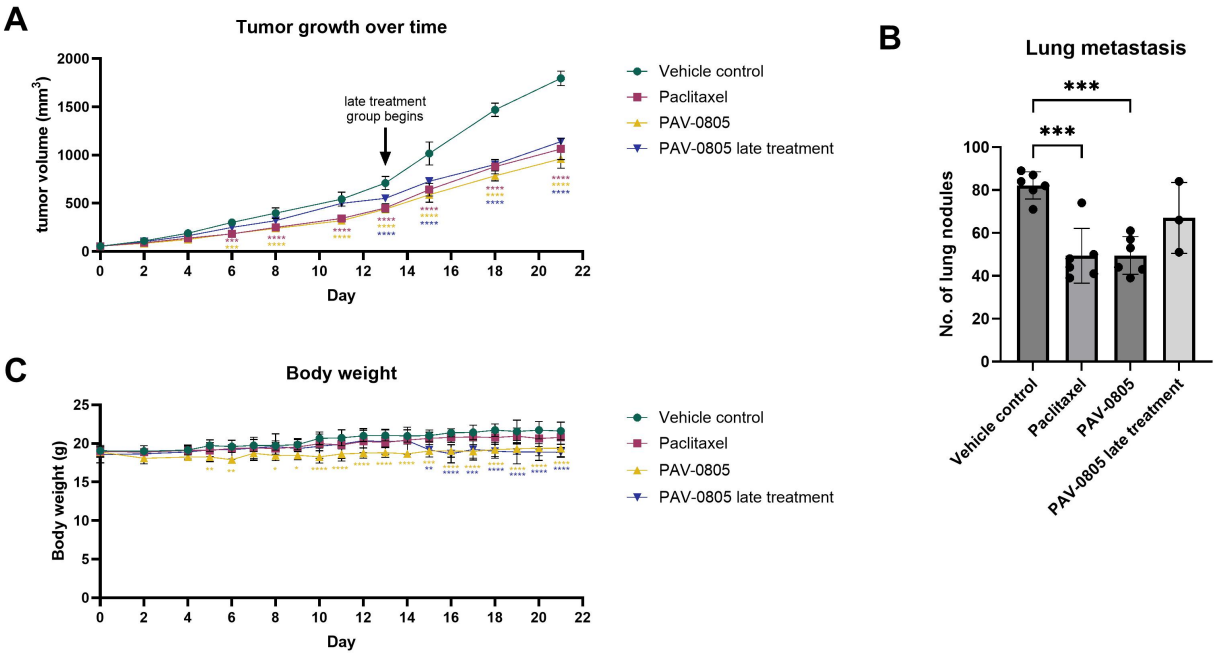

Figure 3. Efficacy of PAV-0805 in the 4T1 allograft model. 4T1 is an aggressive triple-negative mouse breast cancer cell line which spontaneously metastasizes when implanted in mice. In the allograft study, 4T1 tumors were implanted into immunocompetent mice which were then treated with vehicle, 2 mg/kg Paclitaxel, or 10 mg/kg PAV-0805 given beginning when the tumor volume was 50mm^3 or 500mm^3. **Figure 3A** shows growth of the primary tumor over time, with statistical significance indicated based on 2-way anova and Dunnet's multiple comparisons test. **Figure 3B** shows quantitation of lung metastasis upon completion of the study with statistical significance indicated based on one-way anova and Dunnet's multiple comparisons test. **Figure 3C** shows

body weight of mice during the study, with statistical significance indicated based on 2-way anova and Dunnet's multiple comparison test.

Pan-Cancer Activity by Targeting the Hallmarks of Cancer

PAV-951, the parent compound from the pan-cancer assembly modulator series, was determined to target a multi-protein complex. PAV-951 was coupled to a resin, incubated with cancer cell extract, washed 100x to remove non-specifically bound proteins, and then eluted overnight with free drug. The eluates were sent for tandem mass spectrometry (MS-MS) analysis. Eighty-seven proteins were identified by MSMS in triplicate-repeat eluate samples[1]. The identified proteins were then searched in a cancer hallmarks database[27].

The hallmarks database identifies gene sets which are associated with the ten classic hallmarks of cancer— replicative immortality, reprogramming energy metabolism, resisting cell death, tumor promoting inflammation, tissue invasion and metastasis, sustained angiogenesis, evading immune destruction, evading growth suppressors, genome instability, and sustaining proliferating signaling[27–29]. Significant enrichment was found for the hallmarks of reprogramming energy metabolism ($p= 0.001$) and resisting cell death ($P=0.0001$) in the PAV-951 target (see **Figure 4**, left hand side modified from Menyhart et. al.)

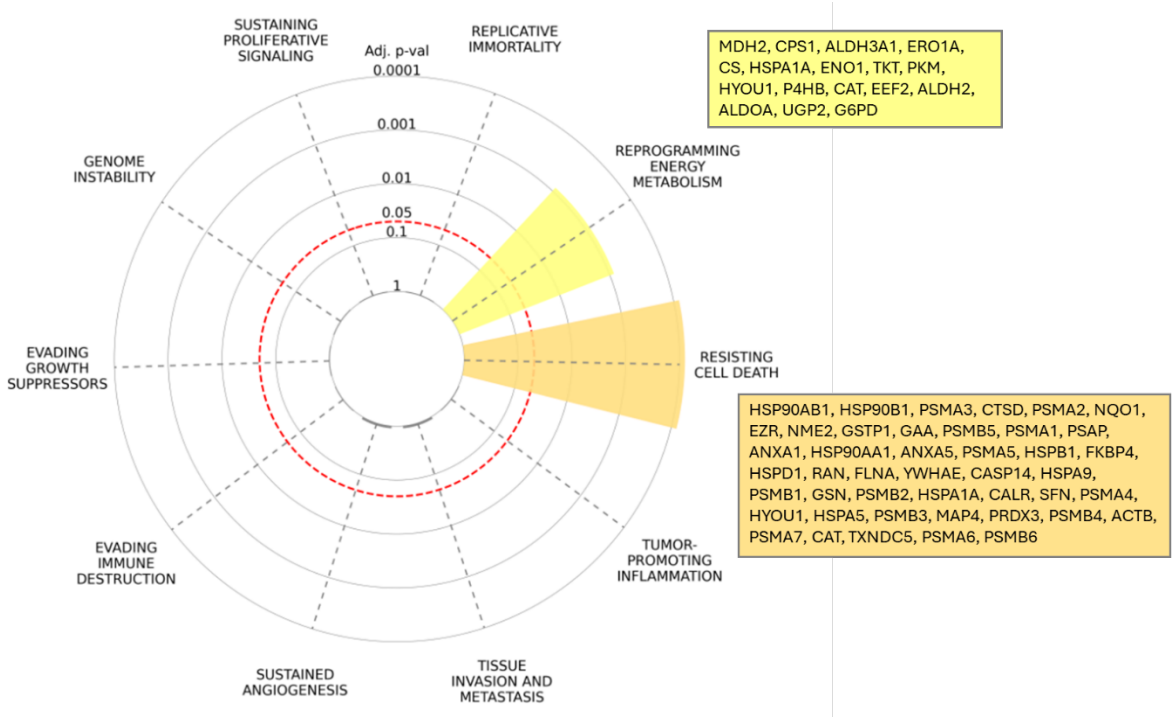

Figure 4. Association of PAV-951 target complex with the Hallmarks of Cancer. Proteins identified by MSMS as comprising the target of PAV-951 were searched in a database for sets of genes associated with the hallmarks of cancer[27]. Association with a particular cancer hallmark is based on the enrichment of hallmark-associated genes identified relative to a reference set. Significant enrichment was found for the cancer hallmarks of reprogramming energy metabolism and resisting cell death. The boxes on the right indicate the proteins identified by MSMS in the PAV-951 resin eluate which are associated with these hallmarks.

Discussion

PAV-951, the original assembly modulator with pan-cancer activity, showed broad but modest activity against the NCI-60 tumor cell panel and in the xenograft mouse models for A549 lung cancer and HT29 colon cancer[1]. SAR exploration demonstrated that small changes to the chemical structure of PAV-951 could eliminate or expand upon the anti-cancer activity. Multiple analogs were identified with no

anti-cancer activity whatsoever, indicating specificity for the active structures. Multiple analogs were identified which eliminated every single tumor line examined. The SAR showing improved safety among analogs with comparably potent anti-tumor cytotoxicity which indicates that toxicity to healthy cells is not an inherent feature of the assembly modulator anti-cancer mechanism.

PAV-0805 is an advanced analog of PAV-951 that shows improved activity against a broader range of cancer cell lines in the NCI-60 screen without toxicity to healthy PBMCs, and significantly inhibited tumor growth and reduced metastasis in the 4T1 allograft model for triple negative, metastatic breast cancer. The anti-cancer effects were significant even when treatment began late and the tumor was already in its exponential growth phase. While PAV-0805 inhibited tumor growth and number of lung nodules without fully eliminating them, its inhibition of tumor growth slightly outperformed Paclitaxel, which is a first-line treatment for metastatic breast cancer in humans[30]. PAV-0805 stands out from other compounds thus far identified in the lead series, including PAV-951, because of its safety. We believe continued optimization of the chemistry through analog exploration will likely result in further improvement. Nevertheless, the enhanced safety already achieved with PAV-0805 concomitant with activity against 4T1, with striking safety on human PBMCs, suggests the chemical series is ready for completion of a Target Product Profile (TPP), the next step before initiation of IND-enabling GLP toxicology as a candidate for human therapeutics.

The enhanced safety observed for PAV-0805 with maintenance of efficacy, is consistent with our working hypothesis on the normal to aberrant assembly machine transition in the development of cancer. The powerful tools available to molecular biology today are not able to parse small subsets of any given gene product that may be distinctive in terms of biological activities. Yet, so called “moonlighting” functions identified to date suggest that proteins are far more heterogeneous than genome sequence alone can reveal[31–34]. Whether due to covalent post-translational modifications, intrinsically unfolded domains, or alternate pathways of protein biogenesis, there is growing recognition that gene expression needs to be parsed in a more granular fashion[34–38]. Viruses appear to have used natural selection to do this in their

struggle with their hosts. We, in turn, used what our phenotypic screen gleaned from viruses to identify starting points for anti-cancer drug discovery.

The MSMS results revealing enrichment in specific cancer hallmark-associated gene products for PAV-951 provides context regarding which cancer-associated biochemical pathways are impacted by assembly modulation. The enrichment analysis showed that the proteins found to be targeted by PAV-951 were associated with the cancer hallmarks of resisting programmed cell death and reprogramming energy metabolism[1,27–29]. Targeting of these cancer hallmarks may explain the observed novel pan-cancer activity of the compounds starting with the PAV-951 parent and more advanced analogs culminating to date in PAV-0805. The unique target and mechanism may be a path to solving the puzzle on developing a treatment which broadly kills cancer cells without killing healthy cells.

Resisting programmed cell death is a fundamental hallmark of cancer[28,29]. Restoring the crucial control points that allow inappropriately proliferating cells to be driven to programmed cell death provides a broad and potent anti-cancer mechanism. Future studies will focus on precisely how that reversal is achieved and how it interfaces with those pathways that are currently far better understood.

Gene products implicated in reprogramming energy metabolism represent a second cancer hallmark enriched in the PAV-951 drug resin eluate. It is likely not a co-incidence that metabolic reprogramming is implicated in viral infection as well[16,39–41]. Reprogramming energy metabolism is critical for creating a cellular microenvironment that serves the need of both viruses and cancer, allowing each to bypass homeostasis[16,28,39]. Activity against abnormal energy metabolism pathways may also explain the potent activity of our compounds in metastasis models (both in cell culture and in the late-treatment allograft group) as cellular reprogramming is a critical component of the epithelial-to-mesenchymal transition which drives the development of metastasis[42,43]. Finally it should be noted that the target multi-protein complex of PAV-951, as well as other assembly modulator compounds, is both transient and energy-dependent[1,5,24]. Perhaps the involvement of energy metabolism in the aberrant,

cancer-associated form of the target multi-protein complex results in increased stability. Further work will be needed to explore these associations.

We have not yet conducted DRAC with PAV-0805, but we have seen that other analogs of PAV-951 contain overlapping, but distinct, subsets of the proteins observed bound to the parent compound drug resin[1]. It will be informative to do a parallel analysis on resin constructed from PAV-0805, given its improved safety. We hypothesize that the PAV-0805 resin eluate will be similarly enriched for the cancer hallmarks of resisting programmed cell death and reprogramming energy metabolism. Further studies will reveal whether this is due to high affinity to the aberrant cancer-specific multi-protein complex target or due to loss of a separate shared target found in a subset of healthy cells. If the later, than the total number of proteins found selectively bound may be strikingly different. If the former, a largely similar subset bound with higher affinity would be predicted. In tandem with DRAC experiments, photocrosslinking experiments must be done to identify which of the many proteins comprising the multi-protein complex directly binds to the compound, and which are peripherally co-associated. By analogy to other assembly modulators, we hypothesize the drug binding protein to be the same for both PAV-951 and PAV-0805[5].

Several things remain to be done to further optimize and understand the pan-cancer assembly modulator series. PAV-0805 is an advanced analog in terms of achieving a balance of efficacy and safety, but it is not the most potent anti-cancer compound we have identified in the series. Further SAR exploration may be needed identify a compound which retains or further improves the safety observed for PAV-0805 and further improves the efficacy. We have not yet begun to undertake the exhaustive process of off-target liability profiling and GLP toxicology, which are required prior to a human clinical study. Nevertheless, we are encouraged that the results we have seen thus far hold the potential to yield a non-toxic cure for cancer, through a novel mechanism.

Methods

National Cancer Institute 60 Cell Line Screen

In the NCI-60 screen, up to 60 cancer cell lines (CCRF-CEM, HL-60(TB), K-562, MOLT-4, RPMI-8226, SR, A549/ATCC, EKVX, HOP-62, HOP-92, NCI-H226, NCI-H23, NCI-H322M, NCI-H460, NCI-H522, COLO 205, HCC-2998, HCT-116, HCT-15, HT29, KM12, SW-620, SF-268, SF-295, SF-539, SNB-19, SNB-75, U251, LOX IMVI, MALME-3M, M14, MDA-MB-435, SK-MEL-2, SK-MEL-28, SK-MEL-5, UACC-257, UACC-62, IGROV1, OVCAR-3, OVCAR-4, OVCAR-5, OVCAR-8, NCI/ADR-RES, SK-OV-3, 786-0, A498, ACHN, CAKI-1, RXF 393, SN12C, TK-10, UO-31, PC-3, DU-145, MCF7, MDA-MB-231/ATCC, HS 578T, BT-549, T-47D, MDA-MB-468) are grown.

Two methods have been used to assess anti-tumor cytotoxicity in the NCI-60 screen.

In the Classic Screen (method used through September 2023), cells were grown for 24 hours then treated with vehicle or compound, or fixed in situ with TCA, to represent a measurement of the cell population for each cell line at the time of drug addition. The treated cells were grown for an additional 48 hours before being fixed in situ with TCA. Fixed cells were then stained with Sulforhodamine B. Absorbance was read to determine cell viability of compound-treated cells relative to both the time at which treatment began and to untreated cells at the end of the study. The NCI-60 screen was initially conducted at a single dose of 2.5uM, but was subsequently repeated with a dose titration.

The human tumor cell lines of the cancer screening panel are grown in RPMI 1640 medium containing 5% fetal bovine serum and 2 mM L-glutamine. For a typical screening experiment, cells are inoculated into 96 well microtiter plates in 100 µL at plating densities ranging from 5,000 to 40,000 cells/well depending on the doubling time of individual cell lines. After cell inoculation, the microtiter plates are incubated at 37° C, 5 % CO_2, 95 % air and 100 % relative humidity for 24 h prior to addition of experimental drugs.

After 24 h, two plates of each cell line are fixed in situ with TCA, to represent a measurement of the cell population for each cell line at the time of drug addition (Tz). Experimental drugs are solubilized in dimethyl sulfoxide at 400-fold the desired final maximum test concentration and stored frozen prior to use. At the time of drug addition, an aliquot of frozen concentrate is thawed and diluted to twice the desired final maximum test concentration with complete medium containing 50 µg/ml gentamicin

Following drug addition, the plates are incubated for an additional 48 h at 37°C, 5 % CO2, 95 % air, and 100 % relative humidity. For adherent cells, the assay is terminated by the addition of cold TCA. Cells are fixed in situ by the gentle addition of 50 µl of cold 50 % (w/v) TCA (final concentration, 10 % TCA) and incubated for 60 minutes at 4°C. The supernatant is discarded, and the plates are washed five times with tap water and air dried. Sulforhodamine B (SRB) solution (100 µl) at 0.4 % (w/v) in 1 % acetic acid is added to each well, and plates are incubated for 10 minutes at room temperature. After staining, unbound dye is removed by washing five times with 1 % acetic acid and the plates are air dried. Bound stain is subsequently solubilized with 10 mM trizma base, and the absorbance is read on an automated plate reader at a wavelength of 515 nm. For suspension cells, the methodology is the same except that the assay is terminated by fixing settled cells at the bottom of the wells by gently adding 50 µl of 80 % TCA (final concentration, 16 % TCA).

In the HTS384 Screen (method used after September 2023), the sixty human tumor cell lines of the cancer screening panel are grown in RPMI 1640 medium containing 5% fetal bovine serum and 2 mM L-glutamine. To initiate a screen, 40 µl of cells are inoculated into the wells of white 384-well microtiter plates at plating densities ranging from 250 to 2,500 cells/well, depending on the doubling time of individual cell lines. After inoculation, the microtiter plates are incubated at 37°C with 5% CO^2 and 95% relative humidity for 24 h before the addition of controls and test agents. Prior to a screen, the test agents and controls are solubilized in dimethyl sulfoxide (DMSO) at 400-fold the final test concentration and stored frozen in polypropylene 384-well microtiter plates.

Twenty-four hours after cell line inoculation, acoustic dispensing is used to transfer 100 nl of DMSO (0.25% (v/v), final) into the wells of microtiter plates, each containing a single cell line. Subsequently, 40 µl of CellTiter-Glo are dispensed into the wells, according to the manufacturer's protocol. Luminescence is measured to assess cell viability at the time of drug addition (time zero, Tz). Acoustic dispensing is also used to transfer 100 nl of controls and test agents (400-fold dilution, final) into duplicate microtiter plates for each cell line to achieve technical replicates. Controls in each microtiter plate include vehicle, 100% cytotoxicity (1 µM Staurosporin NSC755774 and 3 µM Gemcitabine NSC613327 [n = 8]), and five concentrations of doxorubicin (NSC123127, 25 µM [n = 2], 2.5 µM [n = 1], 250 nM [n = 2], 25 nM [n = 1], 2.5 nM [n = 2]. Following the delivery of controls and test agents, the microtiter plates are incubated for 72 h at 37°C with 5 % CO^2 and 95% relative humidity. After 72 h of exposure, 40 µl of CellTiter-Glo are dispensed into the wells of the microtiter plates and luminescence is measured, according to the manufacturer's protocol, to assess cell viability.

For both methods, using the seven absorbance measurements [time zero, (Tz), control growth, (C), and test growth in the presence of drug at the five concentration levels (Ti)], the percentage growth is calculated at each of the drug concentrations levels. Percentage growth is calculated as:

[(Ti-Tz)/(C-Tz)] x 100 for concentrations for which Ti>/=Tz

[(Ti-Tz)/Tz] x 100 for concentrations for which Ti<Tz.

Three dose response parameters are calculated for each experimental agent. Growth inhibition of 50 % (GI50) is calculated from [(Ti-Tz)/(C-Tz)] x 100 = 50, which is the drug concentration resulting in a 50% reduction in the net protein increase (as measured by SRB staining) in control cells during the drug incubation. The drug concentration resulting in total growth inhibition (TGI) is calculated from Ti = Tz. The LC50 (concentration of drug resulting in a 50% reduction in the measured protein at the end of the drug treatment as compared to that at the beginning) indicating a net loss of cells following treatment is calculated from [(Ti-Tz)/Tz] x 100 = -50. Values are calculated for each of these three parameters if the

level of activity is reached; however, if the effect is not reached or is exceeded, the value for that parameter is expressed as greater or less than the maximum or minimum concentration tested.

PAV-951, PAV-0383, PAV-0384 were assessed in the Classic Screen. All others were assessed by the HTS384 screen.

Cytotoxicity Assessment on PBMCs and H9 Lymphoma

Healthy human PBMCs and H9 cells were seeded at a density of 5,000 cells/well and treated with either DMSO or compound, at concentrations of 2.5uM, 5uM, 10uM, and 20uM. The cells were incubated at 37oC for 72 hours then cell viability was measured using an AlamarBlue™ assay.

Mouse Safety

For the intraperitoneal MTD study, female Balb/c mice aged 8-10 weeks were randomly divided into treatment groups with three animals per group. Animals in each treatment group were weighed and received one IP injection of 0.1-0.15mL containing either vehicle (10% DMSO, 45% propylene glycol, 45% sterile water), or varying doses compound. Animals were observed from day 0 until day 3 for clinical signs of toxicity. Animals were euthanized after 72 hours and were examined externally and internally by a pathologist for abnormalities in organ weight and tissue damage. Blood samples were sent for a complete blood count bioanalysis. MTD was determined to be the dose at which no signs of toxicity were observed by any parameters.

Mouse Allograft

A suspension of 0.1×10^6 cells were implanted into the mammary fat pad of normal balb/c mice. Size of the tumor was measured using a digital Vernier caliper. Tumor volume was calculated as the [Length (L) × Width (W) ^{2}] /2, where length (L) is the largest diameter of the tumor and width (W) is the smallest diameter. Animals were treated by IP injection daily with either vehicle (N=6), 2 mg/kg Paclitaxel (N=6), or 10mg/kg PAV-0805 (N=6), beginning when the tumor volume reached $50mm^3$. An additional late treatment group (N=3) received vehicle until the tumor volume reached $500mm^3$, and were subsequently treated with 10mg/kg PAV-0805 daily. Tumor growth inhibition was calculated based on the following formula:

$$\% \text{ TGI} = \frac{\{(TV_{vehicle}\text{ Final} - TV_{vehicle}\text{ Initial}) - (TV_{treatment}\text{ Final} - TV_{treatment}\text{ Initial})\}}{(TV_{vehicle}\text{ Final} - TV_{vehicle}\text{ Initial})} \times 100$$

Animals were sacrificed once the tumor in the vehicle-treated group reached a volume of $2000mm^3$. Lung tissues were isolated and visually observed for metastatic cancer cell colonies.

Drug Resin Affinity Chromatography

A549 cells were grown in minimum essential media (UCSF) with 10% FBS and 1% Penstrep for 48 hours. Cells were scraped into cold phosphate buffered saline (PBS) (10mM sodium phosphate, 150 mM sodium chloride pH 7.4), then spun at 1,000 rpm for 10 minutes until pelleted. The PBS was decanted and the pellet resuspended in a low salt buffer (10mM HEPES pH 7.6, 10mM NaCl, 1mM MgAc with 0.35% Tritonx100) then centrifuged at 10,000 rpm for 10 minutes at 4o C. The post-mitochondrial supernatant was removed and adjusted to a concentration of approximately 5 mg/ml unless otherwise stated and equilibrated in a physiologic column buffer (50 mM Hepes ph 7.6, 100 mM KAc, 6 mM MgAc, 1 mM EDTA, 4mM TGA). The extract was supplemented with an energy cocktail (to a final concentration of 1mM rATP, 1mM rGTP, 1mM rCTP, 1mM rUTP, creatine phosphate and 5 ug/mL creatine kinase). 30 ul

of extract was then incubated for one hour at 22oC on 30 ul of affi-gel resin coupled to PAV-951 or a 4% agarose matrix (control). The input material was collected and the resin was then washed with 3 ml column bufffer. The resins were eluted overnight at 22oC in 100ul column buffer containing 100uM PAV-951 with the energy cocktail. Eluate samples were sent for MSMS analysis.

MSMS Analysis

Samples were processed by SDS PAGE using a 10% Bis-ttris NuPAGE gel with the MES buffer system. The mobility region was excised and washed with 25 mM ammonium bicarbonate followed by 15mM acetonitrile. Samples were reduced with 10 mM dithoithreitol and 60 degrees Celsius followed by alkylation with 5o mM iodacetamide at room temperature. Samples were then digested with trypsin (Promega) overnight (18 hours) at 37 oC then quenched with formic acid and desalted using an Empore SD plate. Half of each digested sample was analyzed by LC-MS/MS with a Waters NanoAcquity HPLC system interfaced to a ThermoFisher Q Exactive. Peptides were loaded on a trapping column and eluted over a 75uM analytical column at 350 nL/min packed with Luna C18 resin (Phenomenex). The mass spectrometer was operated in a data dependent mode, with the Oribtrap operating at 60,000 FWHM and 15,000 FWHM for MS and MS/MS respectively. The fifteen most abundant ions were selected for MS/MS.

Data was searched using a local copy of Mascot (Matrix Science) with the following parameters: Enzyme: Trypzin/P; Database: SwissProt Human (concatenated forward and reverse plus common contaminants); Fixed modification: Carbamidomethyl (C) Variable modifications: Oxidation (M), Acetyl (N-term), Pyro-Glu (N-term Q), Deamidation (N/Q) Mass values: Monoisotopic; Peptide Mass Tolerance: 10 ppm; Fragment Mass Tolerance: 0.02 Da; Max Missed Cleavages: 2. The data was analyzed by label free quantitation (LFQ) and spectral count methods. LFQ intensity values of each condition were measured in triplicate and compared against each other to generate log2 fold change values for each

combination of conditions. Spectral counts were filtered for a 1% protein/peptide false discovery rate requiring 2 unique peptides per protein.

The data set was further adjusted by subtraction of spectral counts for specific proteins observed in the control resin, and subtraction of proteins that were not found in all triplicate-repeat samples. The adjusted dataset was searched for enrichment of cancer hallmarks in the cancerhallmarks.com dataset as described in https://doi.org/10.1016/j.jpha.2024.101065.

References

1. Lingappa, A. F. *et al.* Small molecule protein assembly modulators with pan-cancer therapeutic efficacy. *Open Biol.* **14**, 240210 (2024).
2. Heckmann, C. M. & Paradisi, F. Looking Back: A Short History of the Discovery of Enzymes and How They Became Powerful Chemical Tools. *ChemCatChem* **12**, 6082–6102 (2020).
3. Nirenberg, M. Historical review: Deciphering the genetic code – a personal account. *Trends Biochem. Sci.* **29**, 46–54 (2004).
4. Blobel, G. Protein targeting (Nobel lecture). *Chembiochem Eur. J. Chem. Biol.* **1**, 86–102 (2000).
5. Michon, M. *et al.* A pan-respiratory antiviral chemotype targeting a transient host multi-protein complex. *Open Biol.* **14**, 230363 (2024).
6. Lingappa, U. F. *et al.* Host–rabies virus protein–protein interactions as druggable antiviral targets. *Proc. Natl. Acad. Sci.* **110**, (2013).
7. Reed, J. C. *et al.* Identification of an Antiretroviral Small Molecule That Appears To Be a Host-Targeting Inhibitor of HIV-1 Assembly. *J. Virol.* **95**, e00883-20 (2021).
8. Lingappa, J. R., Hill, R. L., Wong, M. L. & Hegde, R. S. A Multistep, ATP-dependent Pathway for Assembly of Human Immunodeficiency Virus Capsids in a Cell-free System. *J. Cell Biol.* **136**, 567–581 (1997).

9. Du, L. *et al.* A viral assembly inhibitor blocks SARS-CoV-2 replication in airway epithelial cells. *Commun. Biol.* **7**, 486 (2024).

10. Priyamvada, L. *et al.* New methylene blue derivatives suggest novel anti-orthopoxviral strategies. *Antiviral Res.* **191**, 105086 (2021).

11. Reed, J. C. *et al.* HIV-1 Gag co-opts a cellular complex containing DDX6, a helicase that facilitates capsid assembly. *J. Cell Biol.* **198**, 439–456 (2012).

12. Müller-Schiffmann, A., Trossbach, S. V., Lingappa, V. R. & Korth, C. Viruses as 'Truffle Hounds': Molecular Tools for Untangling Brain Cellular Pathology. *Trends Neurosci.* **44**, 352–365 (2021).

13. Javier, R. T. & Butel, J. S. The History of Tumor Virology. *Cancer Res.* **68**, 7693–7706 (2008).

14. Morales-Sánchez, A. & Fuentes-Pananá, E. Human Viruses and Cancer. *Viruses* **6**, 4047–4079 (2014).

15. Krump, N. A. & You, J. Molecular mechanisms of viral oncogenesis in humans. *Nat. Rev. Microbiol.* **16**, 684–698 (2018).

16. Purdy, J. G. & Luftig, M. A. Reprogramming of cellular metabolic pathways by human oncogenic viruses. *Curr. Opin. Virol.* **39**, 60–69 (2019).

17. Münger, K. *et al.* Mechanisms of Human Papillomavirus-Induced Oncogenesis. *J. Virol.* **78**, 11451–11460 (2004).

18. McLaughlin-Drubin, M. E. & Münger, K. The human papillomavirus E7 oncoprotein. *Virology* **384**, 335–344 (2009).

19. Boyer, S. N., Wazer, D. E. & Band, V. E7 protein of human papilloma virus-16 induces degradation of retinoblastoma protein through the ubiquitin-proteasome pathway. *Cancer Res.* **56**, 4620–4624 (1996).

20. White, E. A. *et al.* Systematic identification of interactions between host cell proteins and E7 oncoproteins from diverse human papillomaviruses. *Proc. Natl. Acad. Sci.* **109**, (2012).

21. Flores, E. R., Allen-Hoffmann, B. L., Lee, D. & Lambert, P. F. The human papillomavirus type 16 E7 oncogene is required for the productive stage of the viral life cycle. *J. Virol.* **74**, 6622–6631 (2000).

22. Riley, R. R. *et al.* Dissection of human papillomavirus E6 and E7 function in transgenic mouse models of cervical carcinogenesis. *Cancer Res.* **63**, 4862–4871 (2003).

23. Mir, B. A. *et al.* Increased expression of HPV-E7 oncoprotein correlates with a reduced level of pRb proteins via high viral load in cervical cancer. *Sci. Rep.* **13**, 15075 (2023).

24. Yu, S. F. *et al.* Protein Assembly Modulation: A New Approach to Amyotrophic Lateral Sclerosis (ALS) Therapeutics. *J. Exp. Neurol.* **5**, 210–230 (2024).

25. Yang, Y. *et al.* Immunocompetent mouse allograft models for development of therapies to target breast cancer metastasis. *Oncotarget* **8**, 30621–30643 (2017).

26. Yang, S., Zhang, J. J. & Huang, X.-Y. Mouse models for tumor metastasis. *Methods Mol. Biol. Clifton NJ* **928**, 221–228 (2012).

27. Menyhart, O., Kothalawala, W. J. & Győrffy, B. A gene set enrichment analysis for the cancer hallmarks. *J. Pharm. Anal.* 101065 (2024) doi:10.1016/j.jpha.2024.101065.

28. Hanahan, D. & Weinberg, R. A. The Hallmarks of Cancer. *Cell* **100**, 57–70 (2000).

29. Hanahan, D. & Weinberg, R. A. Hallmarks of Cancer: The Next Generation. *Cell* **144**, 646–674 (2011).

30. Bishop, J. F. *et al.* Paclitaxel as first-line treatment for metastatic breast cancer. The Taxol Investigational Trials Group, Australia and New Zealand. *Oncol. Williston Park N* **11**, 19–23 (1997).

31. Jeffery, C. J. Multitalented actors inside and outside the cell: recent discoveries add to the number of moonlighting proteins. *Biochem. Soc. Trans.* **47**, 1941–1948 (2019).

32. Jeffery, C. J. Protein moonlighting: what is it, and why is it important? *Philos. Trans. R. Soc. B Biol. Sci.* **373**, 20160523 (2018).

33. Jeffery, C. J. Enzymes, pseudoenzymes, and moonlighting proteins: diversity of function in protein superfamilies. *FEBS J.* **287**, 4141–4149 (2020).

34. Jeffery, C. J. Protein species and moonlighting proteins: Very small changes in a protein's covalent structure can change its biochemical function. *J. Proteomics* **134**, 19–24 (2016).

35. Hegde, R. Regulation of protein biogenesis at the endoplasmic reticulum membrane. *Trends Cell Biol.* **9**, 132–137 (1999).

36. Hegde, R. S. & Lingappa, V. R. Membrane Protein Biogenesis: Regulated Complexity at the Endoplasmic Reticulum. *Cell* **91**, 575–582 (1997).

37. Alpert, E. *et al.* Multifunctionality of Prostatic Acid Phosphatase in Prostate Cancer Pathogenesis. *Biosci. Rep.* BSR20211646 (2021) doi:10.1042/BCJ20200944.

38. Uversky, V. N. Dancing Protein Clouds: The Strange Biology and Chaotic Physics of Intrinsically Disordered Proteins. *J. Biol. Chem.* **291**, 6681–6688 (2016).

39. Allen, C. N. S., Arjona, S. P., Santerre, M. & Sawaya, B. E. Hallmarks of Metabolic Reprogramming and Their Role in Viral Pathogenesis. *Viruses* **14**, 602 (2022).

40. Thyrsted, J. & Holm, C. K. Virus-induced metabolic reprogramming and innate sensing hereof by the infected host. *Curr. Opin. Biotechnol.* **68**, 44–50 (2021).

41. Liu, X., Zhu, C., Wang, Y., Wei, F. & Cai, Q. KSHV Reprogramming of Host Energy Metabolism for Pathogenesis. *Front. Cell. Infect. Microbiol.* **11**, 621156 (2021).

42. Faubert, B., Solmonson, A. & DeBerardinis, R. J. Metabolic reprogramming and cancer progression. *Science* **368**, eaaw5473 (2020).

43. Morandi, A., Taddei, M. L., Chiarugi, P. & Giannoni, E. Targeting the Metabolic Reprogramming That Controls Epithelial-to-Mesenchymal Transition in Aggressive Tumors. *Front. Oncol.* **7**, (2017).

Acknowledgements

We thank the National Cancer Institute for running the NCI-60 screening data shown.

Funding

Support for these studies was provided by Prosetta Biosciences, Inc.